Proceedings of the ASME 2010 3rd Joint US-European Fluids Engineering Summer Meeting and 8th International Conference on Nanochannels, Microchannels, and Minichannels
FEDSM-ICNMM2010
August 1-5, 2010, Montreal, Canada

FEDSM-ICNMM2010-30023

NUMERICAL ANAYSIS OF A THERMOPNEUMATIC MICROPUMP

S. Shahsavari
MSc Student
Department of Mechanical Engineering
Sharif University of Technology
shahsavari@mech.sharif.edu

M.B. Shafii
Assistant Professor
Department of Mechanical Engineering
Sharif University of Technology
behshad@sharif.edu

M.H. Saidi
Professor
Department of Mechanical Engineering
Sharif University of Technology
saman@sharif.edu

ABSTRACT

Thermopneumatic micropump is one type of positive displacement micropump, which has many applications due to its relatively large stroke volume, low working voltage, and simple fabrication in microscale. In this paper, a numerical study of heat transfer and fluid flow in a valveless thermopneumatically driven micropump is presented. For rectifying the bidirectional flow, a nozzle and a diffuser are used as the inlet and outlet channels of the chamber. Since the fluid flow is induced by the motion of a diaphragm, the numerical simulation includes fluid structure interaction, which requires applying a dynamic mesh. The domain of solution is divided into two sections; the actuator unit, which contains the secondary fluid, and the main chamber through which the working fluid is passing. The temperature distribution, the pressure variations, and the center deflection of the diaphragm are obtained. In order to validate the model, the numerical results are compared with some experimental data, which shows fair consistency. According to the results of the three dimensional simulation, the rectification efficiency for the nozzle and diffuser channels depends on the frequency.

NOMENCLATURE

c_p	=	Specific heat
E	=	Elasticity
k	=	Conductivity
P	=	Pressure, N/m^2
r	=	Radius
R_{air}	=	Air ideal gas constant
T	=	Temperature, K
t	=	Diaphragm thickness
u	=	Velocity, m/s
V	=	Volume
y	=	Diaphragm deflection
y_0	=	Diaphragm center deflection

Greek symbols

η	=	Diodicity
μ	=	Viscosity, $N.s/m^2$
ξ	=	Pressure loss coefficient
ρ	=	Density, kg/m^3
υ	=	Poisson ratio
χ	=	Rectification efficiency

Subscript

D	=	Diaphragm
rel	=	Relative
w	=	Working fluid

INTRODUCTION

One type of positive displacement micropump is the thermopneumatic micropump having applications in drug delivery systems and bio-chemical analyses.

The major components of a thermopneumatic micropump are i) the main chamber containing the working fluid, ii) the actuator chamber containing a secondary fluid and a resistor heater, and iii) the rectifying elements [1].

Thermopneumatic actuation is based on the volume change of the fluid in the actuator chamber. By heating this fluid expands and deflects the diaphragm. The suction stroke occurs when the heater is inactive. This cycle repeats and as a result a pulsating flow is induced in the chamber. In order to rectify the bidirectional flow,

In most micropumps air is used as the secondary fluid as a result of its simple application.
The time response of thermopneumatic micropums is limited by the rate of heat transfer to and from the secondary fluid. Therefore, these micropumps operate at low frequencies. The main advantages of thermopneumatic actuators are simple fabrication, low operating voltage, and high stroke volume. However, energy consumption is high, and high temperature is one of the problems.
Several experimental works have been done on different types of micropumps, techniques of fabrication, and parametric studies [3-7]. However, there a few studies dedicated to analytical or numerical investigation of these devices. Specially, regarding the heat transfer in thermopneumatic micropumps, there is not much work in literature.
In this paper heat transfer and fluid flow are simulated in a nozzle-diffuser thermopneumatic micropump. Temperature distribution is obtained in different layers of the pump. The net volumetric flow rate is compared to the experimental data of [3].

GEOMETRIC MODEL

The schematic of the micropump to be modeled is shown in figure1. In this micropump, the working fluid is methanol and the secondary fluid is air. The diaphragm diameter is 3.5 mm, the depth of the main chamber and actuator chamber are both 130 μm, the throat width of the diffuser is 80 μm, the length of the nozzle and diffuser channels are 1500 μm, and the divergence angle is 10°. Also the diaphragm thickness is 770 μm. Operating voltage and heater resistance are 50V and 6.54KΩ respectively.

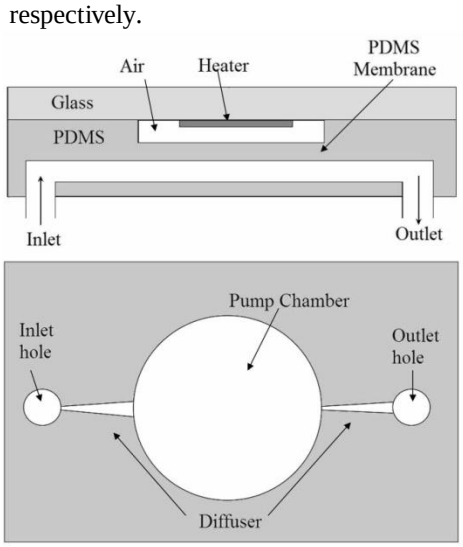

FIGURE 1. SCHEMATIC OF THE MICROPUMP

GOVERNING EQUATIONS

In order to determine the equations governing the fluid flow, first the flow regime should be specified. Fluid flow in micro scales is influenced due to the increase in viscous forces and the flow regime can vary from continuous flow to free-molecular flow. In gas flows, the flow regime can be specified by the Knudsen number, which is defined as the ratio of the molecular mean free path to some characteristic length [2]. Liquids, however, do not have a well-advanced molecular-based theory as dilute gases do. There is no parameter Knudsen number for liquid flows based on which the flow regime can be verified. Under most circumstances, the incompressible Navier–Stokes equations describe liquid flows. In this study, regarding the dimensions of the micropump, the flow regime is continuous for pumping air, which ensures that liquid flow regime in this pump is continuous. For the continuous flow of an incompressible fluid, the mass conservation, momentum principle, and energy equation are as follows

$$\frac{\partial u_k}{\partial x_k} = 0 \tag{1}$$

$$\rho\left(\frac{\partial u_i}{\partial t} + u_k \frac{\partial u_i}{\partial x_k}\right) = -\frac{\partial P}{\partial x_i} + \frac{\partial}{\partial x_k}\left[\mu\left(\frac{\partial u_i}{\partial x_k} + \frac{\partial u_k}{\partial x_i}\right)\right] + \rho g_i \tag{2}$$

$$\rho c_p\left(\frac{\partial T}{\partial t} + u_k \frac{\partial T}{\partial x_k}\right) = \frac{\partial}{\partial x_k}\left(\kappa \frac{\partial T}{\partial x_k}\right) + \frac{1}{2}\mu\left(\frac{\partial u_i}{\partial x_k} + \frac{\partial u_k}{\partial x_i}\right)^2 \tag{3}$$

As the flow is continuous, we have no slip and no temperature jump over the wall. Therefore, the boundary condition for velocity field is $u_{fluid}\,(\text{at wall}) = u_{wall}$ and for temperature field is $T_{fluid}\,(\text{at wall}) = T_{wall}$. The initial conditions for temperature and pressure are the ambient temperature and atmospheric pressure. The initial pressure difference between the inlet and outlet channels is considered to be zero, however, this pressure difference will change as the diaphragm moves up and down and the fluid enters and exits the chamber.
Notice that in this micropump the domain of the solution varies by time the diaphragm deforms as it undergoes the pressure change in the secondary fluid therefore we need to predict the diaphragm motion.
One challenging issue in modeling diaphragm micropumps is considering the fluid-structure interaction (FSI). When the contact surface moves or deforms, the spatial domain occupied by the fluid changes by time and the model should be capable of describing it. This aspect requires applying a dynamic mesh that can be updated at each time step in order to trace the contact surface.
To approach this goal in our simulation, first the diaphragm motion should be obtained from the related governing equations and then the boundary condition for the fluid domain on the deforming wall should be applied from the deflection profile of the diaphragm.

Diaphragm Motion

The deflection curve of a circular diaphragm, clamped at its perimeter and subjected to a pressure load is obtained from [2]:

$$y(r) = y_0[1 - (\frac{r}{R_D})^2]^2 \tag{4}$$

where, y_0 is the center deflection of the diaphragm and R_D is the diaphragm radius. Equation (4) shows that the center deflection of the diaphragm is the key parameter to describe the motion of any point on the diaphragm. Therefore, we only need to seek the transient profile of the diaphragm center deflection.

The relation between the relative pressure applied to the diaphragm, P_{rel}, and the center deflection of a circular diaphragm without pre-stress, y_0, can be estimated as [2]:

$$P_{rel} = P_{air} - P_w = \frac{16 t_D y_0}{3 R_D^{\ 4}} \frac{E}{1-\upsilon^2} (t_D^{\ 2} + \frac{16}{35} y_0^{\ 2}) \qquad (5)$$

Where E, υ, and t_D are the Young's modulus, the Poisson ratio, and the thickness of the diaphragm, respectively. In thermopneumatic micropumps, the applied pressure on the diaphragm is the difference between the air pressure in the pneumatic chamber, P_{air}, and the working fluid pressure P_w, which is assumed to be constant here.

Regarding equation (5), the instantaneous pressure in the actuator chamber is required for determining the center deflection of the diaphragm. Assuming air as an ideal gas and by integrating of equation (4) and obtaining the stroke volume as $\Delta V = \frac{\pi}{3} y_0 R_D^{\ 2}$, we have the equation of state as:

$$P_{air}(t) \times (V_0 + \frac{\pi}{3} R_D^{\ 2} y_0(t)) = \rho_0 V_0 R_{air} T(t) \qquad (6)$$

As we want to verify the transient temperature and pressure, in this equation the temperature, pressure, and center deflection of the diaphragm are written as functions of time. Initially, the air pressure and the working fluid pressure are equal due to the equilibrium state. Substituting equation (5) in equation (6) yields:

$$\left[P_w + \frac{16 t_D y_0}{3 R_D^{\ 4}} \frac{E}{1-\upsilon^2} (t_D^{\ 2} + \frac{16}{35} y_0^{\ 2}) \right] \times (V_0 + \frac{\pi}{3} R_D^{\ 2} y_0(t)) = \rho_0 V_0 R_{air} T(t) \qquad (7)$$

In the left hand side of the above equation, we have a polynomial of degree four and in the right we have a function of time. As a result, provided that the instantaneous temperature is known, the diaphragm center deflection will be determined by solving equation (7). In hydrodynamic simulation, this deflection profile should be applied as the deforming wall boundary condition. The general form of the equation governing the motion of the diaphragm in thermopneumatic micropumps is simplified as:

$$a_4 y_0^{\ 4} + a_3 y_0^{\ 3} + a_2 y_0^{\ 2} + a_1 y_0 + a_0 = T(t) \qquad (8)$$

where the factors a_o to a_4 can be extracted from equation (7) and depends on the geometry, the diaphragm elasticity, and the working fluid pressure.

THERMAL SIMULATION

A thermopneumatic micropump is composed of different layers. The mechanism of heat transfer in these layers is thermal conduction. Due to the dimensions of the micropump and the high aspect ratio of the cylindrical chamber, scale analysis of the energy equation shows that the temperature gradient in the direction perpendicular to the diaphragm is much higher than the two other directions. Therefore, the heat transfer can be considered one dimensional and as a result the thermal problem to be solved is conduction heat transfer in a multi-layered wall.

As can be seen in figure (1), the micropump consists of six layers: glass, ITO heater, air, PDMS diaphragm, water, and PDMS substrate.

There are six decoupled partial differential equations with coupled boundary conditions. The boundary condition to be applied is the continuity of heat flux and temperature on the interface of each two layers. This system of equations is discretized and solved numerically using C++.

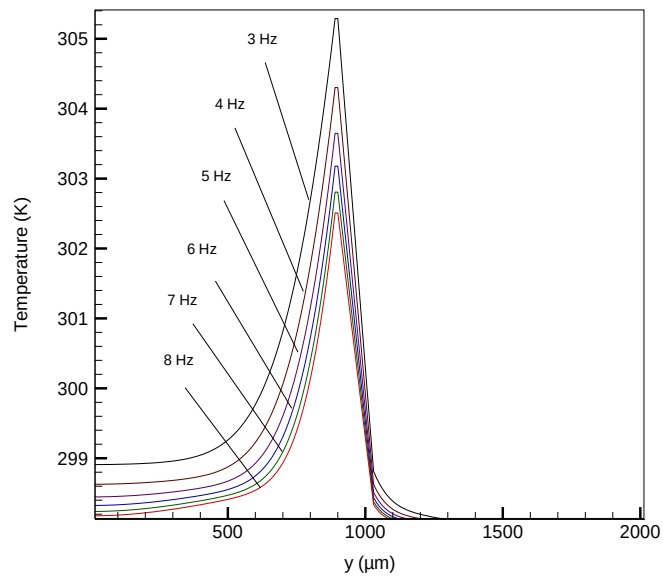

FIGURE 2. ONE DIMENSIONAL TEMPERATURE DISTRIBUTION

Figure 2 shows the temperature distribution in the micropump at the end of heating cycle for different frequencies. In this figure, different layers of the micropump in y direction are: 1) 0 to 900 μm: glass, 2) 900 to 1030μm: air, 3) 1030 to 1730 μm: PDMS diaphragm, 4) 1730 to 1860 μm: methanol, and 5) 1860 to 2000 μm: PDMS substrate.

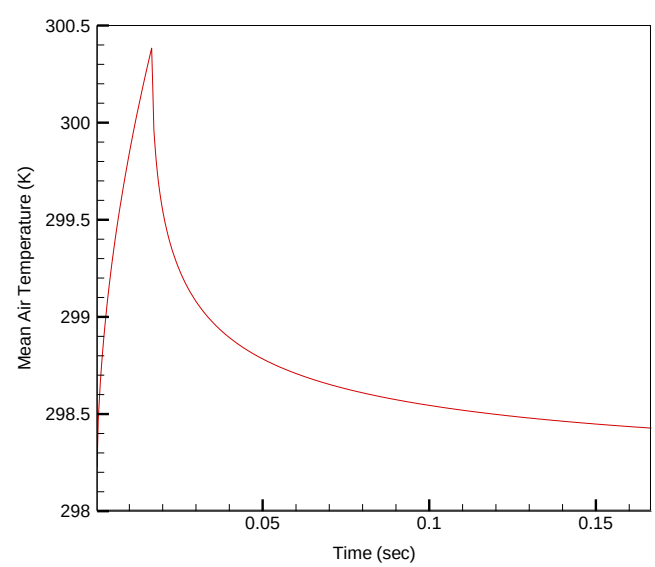

FIGURE 3. AIR TEMPERATURE VARIATION IN ONE CYCLE ($f = 6Hz$)

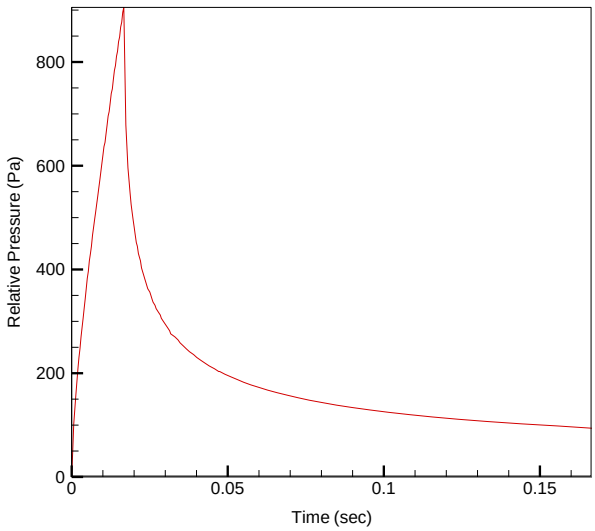

FIGURE 4. AIR RELATIVE PRESSURE VARIATION IN ONE CYCLE ($f = 6Hz$)

Figs. 3 and 4 show the mean air temperature and pressure varying by time during one cycle. The frequency is 6Hz and the duty cycle is 0.1.

Ideally, it is expected that at the end of each cycle all conditions like temperature and diaphragm deflections return back to their initial state. However, theoretically, infinite time is required for the pump to be cooled down and reach the initial conditions. Therefore, we find that at the end of each cycle the diaphragm deflection will not be zero. As a result, when heat transfer is solved for multiple cycles, the final conditions of each cycle should be applied as the initial condition of the next cycle.

By repeating the cycles, the final temperature and the diaphragm deflection at the end of cycles will increase continuously. Figs. 5 and 6 show the variation of the air temperature and the diaphragm center deflection during 10 cycles.

When the center deflection of the diaphragm at the end of a cycle is equal to the depth of the actuator chamber, the diaphragm touches the chamber floor and the pumping will be stopped.

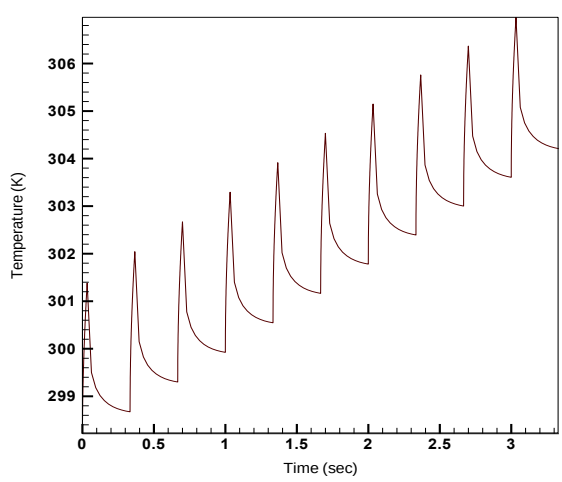

FIGURE 5. AIR MEAN TEMPERATURE VARIATION DURING 10 CYCLES ($f = 3Hz$)

In order to find the maximum number of operating cycles for the micropump, we should continue the solution for multiple cycles until the minimum diaphragm deflection equals to the chamber depth. Using this criterion, the heat transfer equations are solved for multiple cycles in different frequencies. Figure 7 shows the maximum number of operating cycles for the frequencies of the range 3Hz to 8Hz. There is a linear relation between the maximum operating cycles and the frequency. The steep of this line shows the maximum operating time of the micropump, which is constant for all frequencies.

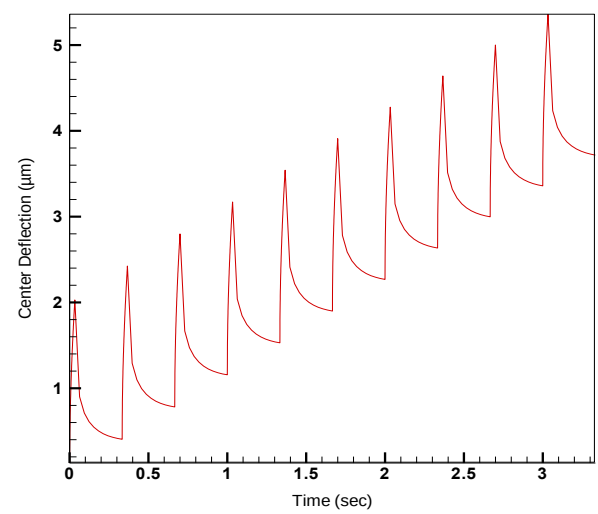

FIGURE 6. DIAPHRAGM CENTER DEFLECTION VARYING DURING 10 CYCLES ($f = 3Hz$)

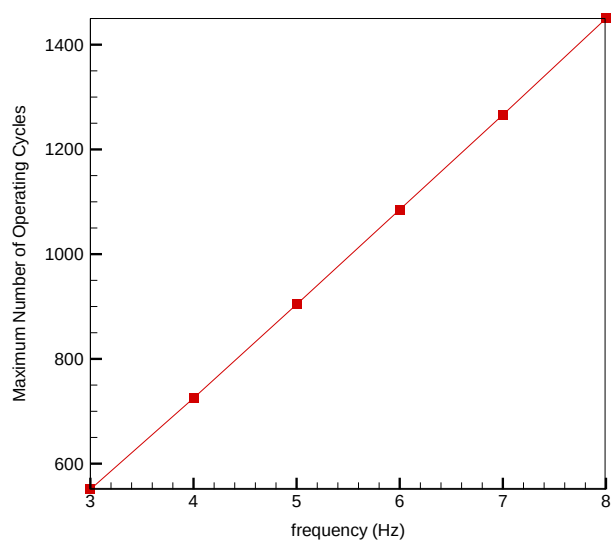

FIGURE 7. MAXIMUM NUMBER OF OPERATING CYCLES

HYDRODYNAMIC SIMULATION

One of the characteristics to be considered in modeling diaphragm micropumps is the fluid-structure interaction. When the contact surface moves up and down, the spatial domain occupied by the fluid deforms. Therefore, in numerical analysis, the mesh should be updated at each time step in order to follow the deflection of the diaphragm.

In our numerical analysis, for solving the momentum and mass conservation equations, we have used FLUENT 6.3.26. The assumptions for our simulation are: laminar, three dimensional, transient flow of isothermal fluid with constant properties.

The first step in the simulation process is solving one dimensional transient heat transfer equations. From the results of this solution, the motion profile of the diaphragm is determined. The next step is applying this as deforming wall boundary condition for the hydrodynamic simulation. The fluid domain is shown in figure 8.

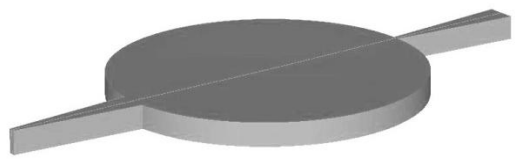

FIGURE 8. FLUID DOMAIN INCLUDING FLUID CHAMBER, NOZZLE, AND DIFFUSER

The flow induced by volume change is a bi-directional pulsatile flow. One simple and efficient method for flow rectification in micropumps is using no moving part valves, such as nozzle- diffuser ones. For small divergence angles, the pressure drop in diffuser direction is less than the pressure drop in nozzle direction.

The pressure loss coefficient ξ for diffuser is defined as:

$$\xi = 2\frac{\Delta p}{\rho \bar{u}^2} \qquad (9)$$

where $\bar{u}$ is the mean velocity in the diffuser neck, ρ is the fluid density, and Δp is the pressure drop across the diffuser. The capability for flow rectification is determined by diodicity, the ratio of pressure loss coefficient in nozzle direction to that in diffuser direction.

$$\eta = \frac{\xi_{nozzle}}{\xi_{diff}} \qquad (10)$$

For rectifying the bi-directional flow, diodicity should be higher than one. For a nozzle-diffuser diaphragm micropump with the stroke volume ΔV and operating frequency f, the volumetric flow rate is obtained by:

$$Q = f.\Delta V.\chi \qquad (11)$$

where χ, the rectification efficiency, is defined by Eq. (12) [10]:

$$\chi = \frac{\sqrt{\eta} - 1}{\sqrt{\eta} + 1} \qquad (12)$$

RESULTS

In our study, we performed the simulation process for the operating frequencies of 3Hz to 8Hz with the duty cycle of 0.1.

Figure 9 shows the transient volumetric flow rate versus τ, the non-dimensionalized time, during one cycle. The negative and positive signs show the flow that exits or enters the chamber, respectively. After 10% of total time of one cycle there is a jump in the plot which is due to the change in the direction of the flow.

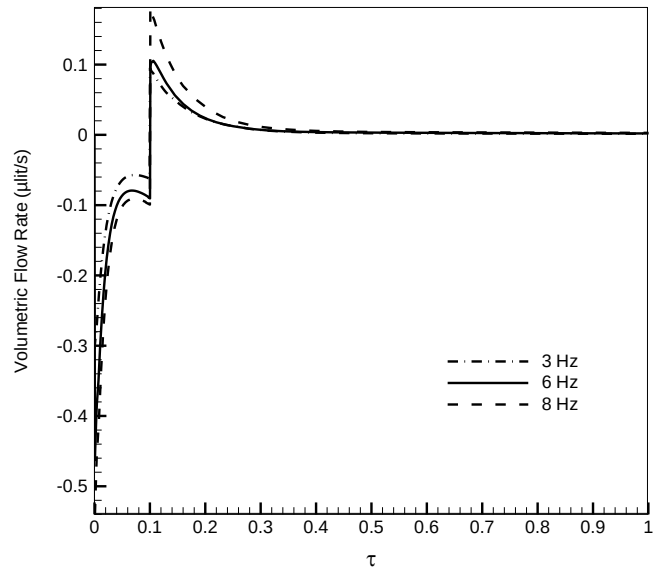

FIGURE 9. VOLUMETRIC FLOW RATE VARYING IN ONE CYCLE

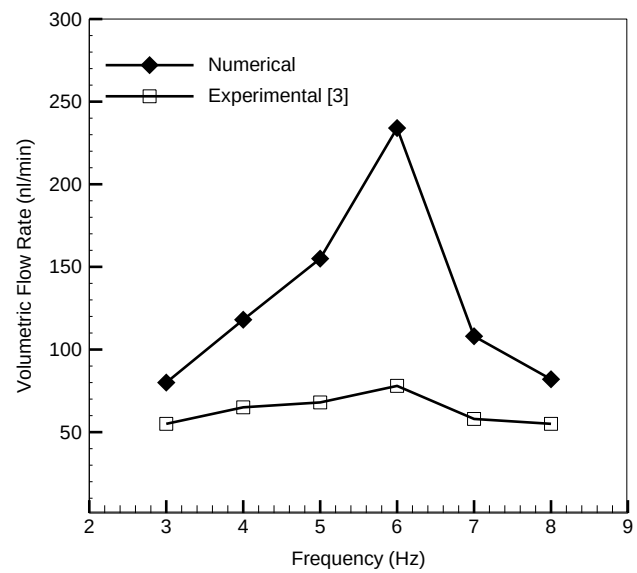

FIGURE 10. NET VOLUMETRIC FLOW RATE

Figure 10 shows the net volumetric flow rate compared to the experimental data presented in [3]. As it can be seen from this figure, in both diagrams the maximum net volumetric flow rate occurs in frequency of 6 Hz, as a result, the optimum frequency is 6Hz.

In Figure 11, the diodicity of nozzle-diffuser is plotted versus frequency. Regarding this plot, both numerical simulation and experimental data prove that diodicity of nozzle-diffuser system depends on actuation frequency. Consequently, the rectification efficiency, which depends on diodicity, is a function of frequency. Here, diodicity is calculated from Eq. (11) by knowing volumetric flow rate, actuation frequency, and stroke volume. Figure 12 shows the rectification efficiency varying by frequency.

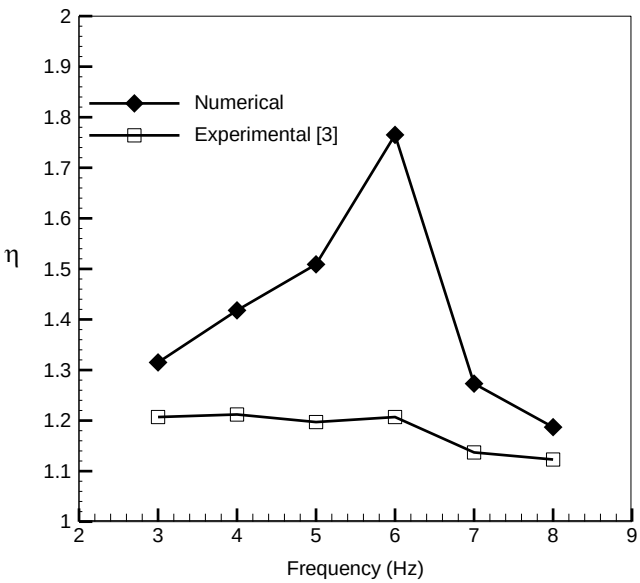

FIGURE 11. DIODICITY VARYING BY FREQUENCY (DUTY RATIO=0.1)

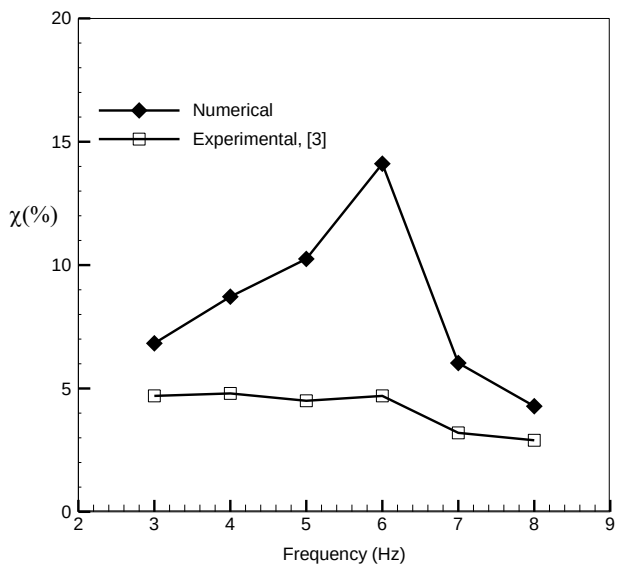

FIGURE 12. RECTIFICATION EFFICIENCY (DUTY ATIO=0.1)

CONCLUSIONS

One of the main applications of thermo-pneumatic micropumps is in drug delivery systems. Due to delicacy of the application, high accuracy in operation is required. Hence accurate and efficient simulation of these devices is essential for their design and fabrication.

In this paper, one dimensional heat transfer in air chamber and fluid chamber of a thermopneumatic micropump was investigated. Moreover, transient air temperature and time dependent deflection profile of diaphragm were obtained. One important result was that the working fluid temperature remains constant during the whole cycle. This is significant in applications where maintaining a constant temperature is of high importance.

Through solving the governing equations for a three dimensional domain, the fluid flow characteristics were studied and the net volumetric flow rate was obtained and compared against the experimental data from open literature. Although the theoretical model overestimated the volumetric flow rate, there was a good consistency in predicting the optimum frequency, where the flow rate is maximized. By hydrodynamic simulation, we found that the rectification efficiency of the nozzle-diffuser channels depends on the frequency. The results of this numerical analysis depend on many parameters, including material of different layers of micropump, voltage and resistance of heater, dimensions of the chambers, diaphragm, and nozzle-diffuser. For future work, parametric studies and design optimization will be considered.

REFERENCES

[1] Laser, D. J., "A Review of Micropumps", Journal of Micromechanics and Microengineering, Vol. 14, pp.35-64, 2004

[2] Nguyen, N.T., "Fundamentals and Application of Microfluidics", 2006

[3] Kim, J., Na, K., Kang, C. J., Kim, Y., "A disposable thermopneumatic-actuated micropum stacked with PDMS layers and ITO-coated glass" Journal of Sensors and Actuators A120 365-369, 2005

[4] Van de Pol, F., Van Lintel, H., Elwenspoek, M., Fluitman, J., "A Thermopneumatic Micropump Based on Micro-engineering Techniques", Journal of Sensors and Actuators A21 -A23 198-202, 1990

[5] Cooney, C.G., Towe, B., "A thermopneumatic dispensing micropump" Journal of Sensors and Actuators A 116 519–524, 2004

[6] Jeong, O., Yang, S., "Fabrication of a Thermopneumatic Micropump with Aluminum Flap Valves", Journal of the Korean Physical Society, Vol. 37, No. 6, December 2000

[7] Jun, D. H., Sim, W. Y., Yang, S. S., "A novel constant delivery thermopneumatic micropump using surface tensions", Journal of Sensors and Actuators, A 139 210-215, 2007

[8] Carmona, M., "Modeling the Thermal Actuation in a Thermo-Pneumatic Micropump", Journal of Electronic Packaging,Vol. 125, 2003

[9] Bejan, A., Kraus, A. D., "Heat Transfer Handbook", John Wiley & Sons, 2003

[10] Sun, C., Yang, Z. H., "Effects of half angle on the flow rectification of a microdiffuser", Journal of Micromechanics and Microengineering. 17, (2007) 2031-2038